Submitted to the Astrophysical Journal
Preprint typeset using LaTeX style emulateapj

CONSTRAINING PRIMORDIAL NON-GAUSSIANITY WITH THE ABUNDANCE OF HIGH REDSHIFT CLUSTERS

James Robinson
Department of Astronomy, University of California, Berkeley CA 94720
Eric Gawiser
Department of Physics, University of California, Berkeley CA 94720
and Joseph Silk
Department of Physics, Astrophysics, 1 Keble Road, University of Oxford, OX1 3NP, UK
and
Departments of Physics and Astronomy, University of California, Berkeley, CA 94720

CfPA Preprint 99-th-02

ABSTRACT

We show how observations of the evolution of the galaxy cluster number abundance can be used to constrain primordial non-gaussianity in the universe. We carry out a maximum likelihood analysis incorporating a number of current datasets and accounting for a wide range of sources of systematic error. Under the assumption of gaussianity, the current data prefer a universe with matter density $\Omega_m \simeq 0.3$, and are inconsistent with $\Omega_m = 1$ at the 2σ level. If we assume $\Omega_m = 1$, the predicted degree of cluster evolution is consistent with the data for non-gaussian models where the primordial fluctuations have at least two times as many peaks of height 3σ or more as a gaussian distribution does. These results are robust to almost all sources of systematic error considered: in particular, the $\Omega_m = 1$ gaussian case can only be reconciled with the data if a number of systematic effects conspire to modify the analysis in the right direction. Given an independent measurement of Ω_m, the techniques described here represent a powerful tool with which to constrain non-gaussianity in the primordial universe, independent of specific details of the non-gaussian physics. We discuss the prospects and strategies for improving the constraints with future observations.

1. INTRODUCTION

Most studies of structure formation in the universe start from the assumption that the primordial perturbations were gaussian. Many well motivated models, however, predict non-gaussian fluctuations, including topological defect models (Kibble 1976; Vilenkin & Shellard 1994), and certain forms of inflation (Peebles 1983,1997,1998a,1998b; La 1991; Amendola & Occhionero 1991; Amendola & Borgani 1993). One area which has recently received a considerable degree of attention in the gaussian case is the evolution of the galaxy cluster number abundance. Several authors (Frenk et al. 1990; Oukbir & Blanchard 1992; Oukbir & Blanchard 1997; Fan, Bahcall & Cen 1997; Gross et al. 1997; Blanchard & Bartlett 1998; Eke et al. 1998; Reichart et al. 1998; Viana & Liddle 1998) have shown how cluster evolution data can be used to constrain the matter density of the universe under the assumption of gaussianity, with most studies favoring a low density universe.

Some attempts have been made to extend studies of cluster formation to the non-gaussian case. Oukbir, Bartlett & Blanchard (1997) noted the existence of a degeneracy between the spectral index of the primordial fluctuations and primordial non-gaussianity. Colafrancesco, Lucchin & Matarrese (1989), and later Chiu, Ostriker & Strauss (1997) have introduced a modified version of the Press-Schechter (1974) formalism to make predictions for the cluster number density in a non-gaussian model, and Robinson, Gawiser and Silk (1998, hereafter RGS98) have generalized this approach. Robinson & Baker (1999) have tested this formalism, and verified that it is able to accurately fit the evolution of the cluster number abundance observed in N-body simulations of structure formation with non-gaussian initial conditions. Various authors (RGS98; van de Bruck 1998; Koyama, Soda & Taruya 1999) have used this formalism to study the evolution and clustering properties of galaxy clusters and thus constrain non-gaussianity in the primordial fluctuations. Willick (1999) has considered the constraints on non-gaussianity which can be derived from the existence of cluster MS1054-03 at a redshift $z = 0.83$. In this paper, we extend previous work by carrying out a detailed study of cluster evolution in the non-gaussian case, performing a Bayesian likelihood analysis, considering a number of different cluster observations, and accounting for a wide range of possible sources of systematic error.

Our results demonstrate that given an independent measurement of the matter density of the universe (which we can realistically expect to gain in the near future from CMB and supernovae observations), cluster evolution data can place strong constraints on non-gaussianity. The greatest strength of our analysis is that it uses observations to place direct constraints on non-gaussianity (in particular, on the probability distribution function, or PDF, of the primordial density field), without any reference to the details of the non-gaussian physics in specific models. Because of the infinite range of possible non-gaussian models and the difficulties in making accurate predictions even in well specified cases, the model independent constraints on non-gaussianity considered here are therefore particularly powerful. In section 2 we discuss the parameterization of our models and the process of predicting the cluster number density at different redshifts. In section 3 we discuss the different datasets used in our analysis and our method

for computing the likelihood of observing a dataset given one of our models. In section 4 we discuss the resulting constraints on non-gaussianity from existing cluster data, the likely sources of systematic error, and the improvement we can hope to gain from future data. In section 5 we draw our conclusions.

2. MODELS

The models we consider are specified by knowledge of the power spectrum of the fluctuations, the nature of the non-gaussianity, the background cosmology, and the cluster mass-temperature relationship. We discuss the parameterization of these properties in the following subsections.

2.1. *Power Spectrum*

We parameterize the power spectrum $P(k)$ for each model using a cold dark matter (CDM) form (Bond et al. 1991), that is

$$P(k) \propto kT^2(k) \tag{1}$$

where

$$T(k) = \frac{\ln(1+2.34q)}{2.34q} \times \left[1+1.389q+(16.1q)^2+(5.46q)^3+(6.71q)^4\right]^{-1/4} \tag{2}$$

and

$$q = \frac{k}{\Gamma h \mathrm{Mpc}^{-1}} \tag{3}$$

Here Γ is the shape parameter (which is well fit by $\Gamma = \Omega_m h \exp(\Omega_\mathrm{B} - \Omega_\mathrm{B}/\Omega_\mathrm{m})$ for both open and flat CDM models, where Ω_m is the contribution of CDM and baryons to the critical density at $z = 0$, Ω_B is the contribution of the baryons, and the Hubble constant is parameterized via $H_0 = 100h\mathrm{km\ s^{-1}Mpc^{-1}}$). Although this form is derived within the context of the CDM model, it can also be used to fit power spectra from a range of structure formation scenarios, at least over the range of scales relevant to cluster formation. We quantify the normalization of the power spectrum by specifying σ_8, the *rms* density fluctuation in spheres of radius $8h^{-1}$Mpc.

2.2. *Non-gaussianity*

Non-gaussianity is specified in terms of the probability distribution function (PDF) $p_R(\delta)$ of the primordial fluctuations, where $p_R(\delta)\,d\delta$ is the probability of the overdensity (linearly extrapolated to a redshift $z = 0$) in a sphere of radius R, having a value between δ and $\delta + d\delta$. For most non-gaussian models, it is reasonable to assume that the PDF is scale invariant over the range of scales relevant to cluster formation (see Robinson & Baker 1999 for specific examples). In this case, we can make use of a rescaled PDF, which we denote $P(y)$, satisfying

$$P(y)\,dy = \frac{1}{\sigma_R} p_R(\delta)\,d\delta \tag{4}$$

where σ_R is the *rms* fluctuation in spheres of radius R.

The rescaled PDF $P(y)$ has a mean of zero and an *rms* of one. For a wide range of models (see Robinson & Baker 1999 for examples) $P(y)$ can be well fit by a log-normal distribution, that is

$$P^A_{LN}(y) = \frac{C}{\sqrt{2\pi A^2}} e^{-x^2(y)/2 - |A|x(y)} \tag{5}$$

where

$$x(y) = \frac{\ln(B + Cy|A|/A)}{|A|} \tag{6}$$

with

$$B = e^{A^2/2} \tag{7}$$

$$C = \sqrt{B^4 - B^2} \tag{8}$$

This distribution has one free parameter A, with the limit $A = 0$ corresponding to gaussianity. Following RGS98, we characterize each PDF in terms of a single non-gaussianity parameter G, where

$$G = 2\pi \frac{\int_3^\infty P(y)dy}{\int_3^\infty e^{-y^2/2}dy}. \tag{9}$$

G is the probability of obtaining a peak of height 3σ or higher for the PDF in question, relative to that for a gaussian model. A value $G > 1$ indicates an excess of large positive fluctuations, $G < 1$ indicates a deficit, while $G = 1$ indicates gaussian fluctuations. Since rich clusters typically form from 3σ or higher peaks in the primordial fluctuations, this parameter is a useful quantifier of non-gaussianity in the context of cluster formation.

2.3. *Background Cosmology*

The background cosmology is specified by two parameters, the fraction of critical density at $z = 0$ contributed by dark matter (Ω_m) and the fraction contributed by a cosmological constant (Ω_Λ). We restrict our investigation to the flat (Ω_m+Ω_Λ=1) and open ($\Omega_\Lambda = 0$) cases.

2.4. *Cluster Mass-Temperature relationship*

The Press-Schechter (PS) formalism (Press & Schechter 1974) allows us to predict the number density of clusters in the universe as a function of cluster mass. This formalism has been adapted to the non-gaussian case, by Colafrancesco, Lucchin & Matarrese (1989), Chiu et al. (1997), and RGS98 and has been shown by Robinson & Baker (1999) to fit the cluster evolution observed in non-gaussian models of structure formation to better than 25% accuracy. In particular, the number density of clusters with masses between M and $M + dM$ is given by

$$n(M)dM = \frac{3f}{4\pi R(M)^3} P[y_c(M)] \frac{d[y_c(M)]}{dM}. \tag{10}$$

Here $R(M)$ is the Lagrangian (pre-collapse) radius of a sphere giving rise to a cluster of mass M, which satisfies

$$M = \frac{4\pi}{3} R(M)^3 \rho_b \tag{11}$$

with ρ_b being the comoving background density of the universe. Also

$$y_c(M) = \delta_c/\sigma_M \tag{12}$$

where σ_M is the *rms* mass fluctuation on scale M, linearly extrapolated to redshift z, and δ_c is the critical overdensity

for collapse, which has the value 1.69 in a flat universe (for fits to the weak cosmological dependence, see Kitayama & Suto 1996). Finally, f is a correction factor, given by

$$f = \frac{1}{\int_0^\infty dy P(y)} \tag{13}$$

which is included to ensure that the mass function accounts for the entire mass of the universe. In the Gaussian case f takes the value two, as originally proposed by Press & Schechter (1974) and explained by Bond et al. (1991) using the excursion set formalism.

The Press-Schechter formalism allows us to accurately predict the cluster number density as a function of cluster mass. For most of the clusters considered in this work we observe not the mass but the temperature of the intracluster medium (via the spectrum of emitted X-rays). We therefore need to make use of a mass-temperature relation in order to compare our models with observations. Hydrodynamical simulations of cluster formation (Navarro, Frenk & White 1995; Evrard, Metzler & Navarro 1996; Eke, Navarro & Frenk 1998) suggest that the relationship between mass and temperature can be well fitted by

$$kT_{gas} = \frac{9.37}{\beta(5X+3)} \left(\frac{M}{10^{15}h^{-1}M_\odot}\right)^{2/3} (1+z) \left(\frac{\Omega_m}{\Omega_z}\right)^{1/3} \Delta_C^{1/3} \mathrm{keV} \tag{14}$$

where Δ_C is the ratio of the mean halo density to the critical density at redshift z (for fitting functions in various cosmologies, see Kitayama & Suto 1996), X is the hydrogen mass fraction (we take $X = 0.76$), and β is the ratio of the specific galaxy kinetic energy to the specific gas thermal energy. Numerical simulations suggest that the average value for this quantity is in the range $\bar{\beta} = 1.0 - 1.3$. For the bulk of this work we take $\bar{\beta} = 1.0$, although we also investigate the effect of varying the value. Unfortunately, knowledge of the mean value of β is not enough to specify our models, as the mass temperature relation is also subject to scatter, with some clusters of a given mass being hotter and other clusters being colder. Simulations suggest that the spread of β values can be reasonably fit as a log-normal distribution, that is $\log_{10}(\beta)$ is gaussianly distributed, with mean $\log_{10}(\bar{\beta})$ and variance σ_β. Using the distribution of β values, we can infer the probability $p(T|M)dT$ of a cluster of mass M having a temperature between T and $T+dT$. The expected number density $n(T)dT$ of clusters with temperature between T and $T+dT$ is then given by

$$n(T)dT = \int p(T|M) n(M) dM \tag{15}$$

Due to the fact that $n(M)$ for typical models is a sharply falling function of M, increasing the scatter σ_β systematically boosts $n(T)$. We adopt $\sigma_\beta = 0.065$ as a fiducial choice, though we also investigate the effect of variations about this value. The additional scatter in the mass-temperature relation caused by temperature measurement errors is typically smaller than the intrinsic scatter discussed above, but we can account for it in the same way by adding temperature measurement errors in quadrature to σ_β.

To summarize, our models are parameterized by 7 parameters: Γ, σ_8, G, Ω_m, Ω_Λ, β and σ_β.

3. DATA

We extract information on the redshift evolution of clusters from three sources:

- Henry & Arnaud clusters: This is an X-ray selected sample of clusters with galactic latitude $b > 20^\circ$ and a flux limit $f_{\rm min} = 3 \times 10^{-11}$erg cm^{-2} s^{-1} in the $2-10$keV band (Henry & Arnaud 1991). The sample contains 25 objects, with a median redshift $z = 0.05$, and is at least 90% complete (for the purposes of this work we shall assume 100% completeness, although it makes no difference to our conclusions).

- *Markevitch clusters:* This is an X-ray selected sample of clusters with $b > 20^\circ$ and cooling-flow corrected flux greater than $f_{\rm min} = 2 \times 10^{-11}$ erg cm^{-2} s^{-1} in the $0.1 - 2.4$keV range (Markevitch 1998). In addition, the sample is volume limited by requiring $z_{\rm min} < z < z_{\rm max}$ with $z_{\rm min} = 0.04$ and $z_{\rm max} = 0.09$. For an explanation of the cooling flow correction procedure, see Markevitch (1998). We make use of both cooling flow corrected and uncorrected temperatures in this analysis.

- *EMSS clusters:* The EMSS clusters are selected from an X-ray survey in the 0.3-3.5keV band covering a total area $A_{\rm tot} = 735$ square degrees. The fraction of survey area A sensitive to fluxes larger than $f_{\rm det}$ can be fit to better than 10% accuracy (Eke et al. 1998) for fluxes greater than 2.5×10^{-13}erg cm^{-2} s^{-1} by

$$\frac{A(f_{\rm det})}{A_{\rm tot}} = 1 - 3.05e^{-0.41 f_{\rm det}} + 2.30e^{-0.77 f_{\rm det}}. \tag{16}$$

  We consider a volume limited sample of 9 clusters with $0.3 < z < 0.4$ whose temperatures have been measured by the ASCA satellite (Henry 97). We also consider a sample comprising two objects with temperatures measured by ASCA (MS0015.9+1609, $z = 0.54$, $kT = 8.0 \pm 0.6$keV, Mushotzky & Scharf 1997; MS0451.6-0305, $z = 0.54$, $kT = 10.4 \pm 1.2$keV, Donahue 1996), for which we take the redshift limits to be $0.5 < z < 0.65$. Finally, we consider another sample comprising one object (MS1054.5-0321, $z = 0.83$, $kT = 14.7 \pm 2.1$keV, Donahue et al. 1998), with redshift limits taken to be $0.65 < z < 0.9$. We will investigate whether this choice of redshift limits affects our results.

We analyze each sample as follows: First, we model the relationship between luminosity (L) and temperature for each sample as a gaussian distribution in $\log(L)$, with mean given by

$$\log_{10}(L_X/(10^{44}\mathrm{erg\ s^{-1}})) = A_1 \log_{10}(kT/\mathrm{keV}) + A_2 \tag{17}$$

and a standard deviation

$$\sigma_L = A_3 \log_{10}(kT/\mathrm{keV}) + A_2 \tag{18}$$

The subscript X denotes the observing band for the sample in question, and fiducial values for the parameters A_1, A_2, A_3 and A_4 for each of the cluster samples are (see Eke et al. 1998): Markevitch $A_1 = 2.1$, $A_2 = -1.485$,

$A_3 = 0.0$, $A_4 = 0.104$; Henry & Arnaud $A_1 = 3.93$, $A_2 = -2.92$, $A_3 = -0.52$, $A_4 = 0.70$; EMSS clusters $A_1 = 3.54$, $A_2 = -2.85$, $A_3 = -0.47$, $A_4 = 0.69$. Having assumed a luminosity-temperature (LT) relation, we compute the average volume $V_{\rm max}(T)$ in which a cluster of temperature T could be seen for the sample in question:

$$V_{\rm max}(T) = \int dL\, p(L|T) \int_{z_{\rm min}}^{z_{\rm max}} dz\, \frac{d^2V}{d\omega dz}\, \omega(L,z)\, \theta(L - 4\pi f_{min} d_L^2(z)) \tag{19}$$

where $p(L|T)$ is the probability distribution of L for a given value of T (defined above), $d^2V/(d\omega dz)$ is the comoving volume element per unit redshift per solid angle, $\omega(L,z)$ is the solid angle associated with flux limit L at redshift z, d_L is the luminosity distance, and $\theta(x)$ is the Heaviside function

$$\theta(x) = \begin{cases} 1 & \dots x \geq 0 \\ 0 & \dots x < 0 \end{cases} . \tag{20}$$

The LT relation for each sample is subject to various uncertainties, and at high redshifts the number of clusters for which luminosity and temperature have been observed is so low that any accurate determination is virtually impossible. For flux limited samples, uncertainties in $p(L|T)$ will lead to uncertainties in $V_{\rm max}$, and therefore to uncertainties in the inferred number density of clusters. However, for surveys which are limited in both flux and volume, sufficiently hot clusters will typically be so bright that for all reasonable luminosities they could be seen throughout the entire survey volume, so the uncertainty in $V_{\rm max}$ is much smaller. We investigate this effect by plotting the cumulative temperature function

$$N_{>T} = \sum_{T_i > T} \frac{1}{V_{\rm max}^i} \tag{21}$$

for the Markevitch and Henry samples discussed above ($N_{>T}$ is the number density of clusters with temperature greater than T, T_i and $V_{\rm max}^i$ are the temperature and maximum volume for the ith cluster in the sample, and the sum runs over all clusters), using four different assumptions about the LT relationship. For "Fiducial LT" we use the LT model and parameters discussed above. For "High LT" we multiply luminosities in the fiducial model by a factor of 10, and for "Low LT" we divide by a factor of 2. For "Actual Luminosities" we use individual luminosities observed for each cluster.

Results for these four cases in a critical density universe are shown in figs. 1 and 2. The Markevitch sample (fig.1), which is volume limited, shows virtually no dependence on the LT relationship for $T > 6.3$keV, and the Henry sample (fig.2) is similarly robust for this temperature range. For the remainder of this work, we will concentrate our analysis on clusters with temperatures $T > 6.3$keV for the low redshift samples, $T > 8.0$keV for the $0.5 < z < 0.65$ sample, and $T > 10$keV for the $0.65 < z < 0.9$ sample. As discussed, restricting our analysis to the highest temperature clusters reduces the dependence of our results on uncertainties in the LT relation. As a consequence, we will not worry about the effect of K-corrections, whose typical effect on the luminosity is less that the uncertainties in the LT relation. An additional advantage of restricting our study to the highest temperature clusters is that heating of the intra-cluster medium by supernovae (which could affect the cluster mass-temperature relation) is likely to be least important in this regime, as discussed by Viana & Liddle (1998).

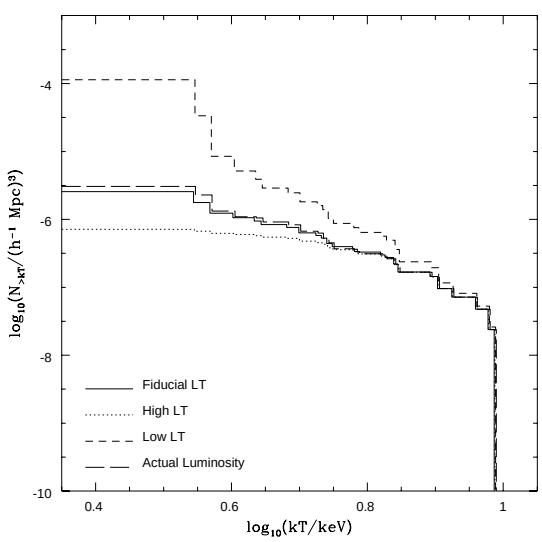

FIG. 1.— Cumulative temperature function for the Markevitch (1998) cluster sample, assuming $\Omega_m = 1$, $\Omega_\Lambda = 0$, and four different versions of the luminosity-temperature relation, as discussed in the text.

We comment briefly on the adopted slope of the LT relation. For the Markevitch sample, we adopt a slope $A_1 = 2.1$ as measured by Markevitch (1998) for the 0.1-2.4 keV observing band. This corresponds to a slope for the bolometric luminosity vs temperature relation of 2.64. We follow Eke et al. (1998) in adopting a slope $A_1 = 3.93$ for the Henry and Arnaud sample, and $A_1 = 3.54$ for the EMSS clusters. Self-similar scaling arguments on the other hand would imply a slope $A_1 = 2$ (Kaiser 1986), while a different study of the low redshift LT relation (Arnaud & Evrard 1998) finds a slope of 2.88. As discussed, our analysis is not strongly affected by uncertainties in the LT relation, and variations of the slope within the range suggested by the observations do not significantly alter our conclusions.

From the above discussion we anticipate that for some range of temperatures $T_{\rm min} < T < T_{\rm max}$, the maximum volume $V_{\rm max}$ will be robust, depending only weakly on uncertainties in the LT relationship. Exploiting this fact, we can make use of a simple expression for the likelihood function: assuming that the clusters are Poisson distributed, the likelihood $\mathcal{L}$ of observing a sample of $N_{\rm c}$ clusters given

a temperature function $n(T)$ is

$$\mathcal{L} = \prod_{i=1\ldots N_c} n(T_i)V_{\max}(T_i) \prod_{j=1\ldots N_b-N_c} (1 - n(T_j)V_{\max}(T_j)) \quad (22)$$

where the temperature range has been divided into a set of N_b bins, the sum i runs over all bins containing a cluster, the sum j runs over all bins not containing a cluster, and the bins are sufficiently small that the probability of finding more than one cluster in a bin is negligible. In the limit that the bin size tends to zero, $\ln \mathcal{L}$ satisfies (up to an additive constant $\mathcal{L}_0$)

$$\ln \mathcal{L} = \sum_i \ln\left(n(T_i)V_{\max}(T_i)\right) - \int_{T_{\min}}^{T_{\max}} n(T)V_{\max}(T)dT + \mathcal{L}_0 \quad (23)$$

where the index i runs over all clusters in the sample satisfying $T_{\min} < T_i < T_{\max}$. Provided $V_{\max}$ is well determined for the range of temperatures we will consider, this expression gives a robust determination of the likelihood. Eke et al. (1998) have used a very similar expression for the likelihood which also takes account of individual redshifts within a cluster sample. However, since the $n(T)$ laws do not change too dramatically within the redshift ranges probed by each of our samples, we choose instead to work just with $n(T)$ for the median redshift of each sample.

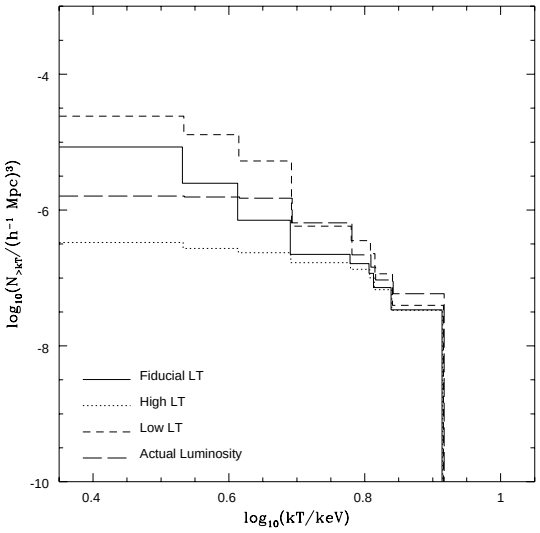

FIG. 2.— Cumulative temperature function for the Henry (1997) cluster sample, assuming $\Omega_m = 1$, $\Omega_\Lambda = 0$, and four different versions of the luminosity-temperature relation, as discussed in the text.

4. RESULTS

4.1. *Current Data*

We now consider in detail the constraints we can place on Ω_m and non-gaussianity using current observational data. As we will see later, the results do not depend strongly on whether the universe is flat or open, so for the time being we will concentrate on the case of an open universe with zero cosmological constant. To start our discussion, we consider the constraints placed by just two of the datasets: the Markevitch data at low redshift, and the $0.65 < z < 0.9$ data containing MS1054.5-0321 at high redshift. Fig.3 shows confidence limits derived by combining these two datasets: in the $\Omega_m - \sigma_8$ plane assuming an open universe with $G = 1$ (left panel), in the $G - \sigma_8$ plane assuming $\Omega_m = 1$ (central panel) and in the $G - \sigma_8$ plane assuming $\Omega_m = 0.3$ (right panel). The solid lines show 90% confidence limits for the Markevitch data, the dotted lines show 90% limits for the $0.65 < z < 0.9$ data, and the dark and light shaded regions show 68% and 90% confidence regions for the combined data sets. Confidence limits are computed assuming uniform priors in all variables. Under the assumption of gaussianity, the combined datasets prefer $\Omega_m \simeq 0.3$ with $\Omega_m = 1$ excluded at more than the 2σ level, though we will see in a moment that various systematic uncertainties might affect this conclusion. A critical universe is consistent with the the two datasets if the fluctuations are non-gaussian with $G \gtrsim 2.5$.

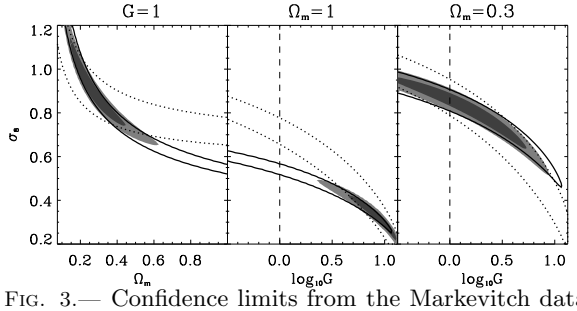

FIG. 3.— Confidence limits from the Markevitch data (solid lines, 90% limits), the $0.65 < z < 0.9$ data (dotted lines, 90% limits), and for the combined data sets (dark shaded region, 68% limits; light shaded region, 95% limits), for the cases $G = 1$ (left panel), $\Omega_m = 1$ (central panel) and $\Omega_m = 0.3$ (right panel). The vertical long-dashed lines in the center and left panels show the location of gaussian fluctuations.

The discussion above, which uses just two of our datasets, illustrates the basic degeneracy (in the $\Omega_m - \sigma_8$ or $G - \sigma_8$ plane) intrinsic to cluster observations at a single redshift, and how this degeneracy is broken using observations of cluster evolution. Before embarking on a full likelihood analysis incorporating all of the datasets, we will check the consistency of the various datasets, and investigate various systematic effects which might alter our conclusions.

First, we consider the effect of using different low redshift data. Fig.4 shows the likelihood (marginalized over σ_8 assuming a uniform prior) for four different choices of low redshift data, for the cases $G = 1$, $\Omega_m = 1$, and $\Omega_m = 0.3$. The low redshift data considered are the Markevitch sample, the Markevitch sample with temperatures not corrected for cooling flows, the Henry and Arnaud sample, and the Henry and Arnaud sample with a redshift limit of $z < 0.09$ imposed.

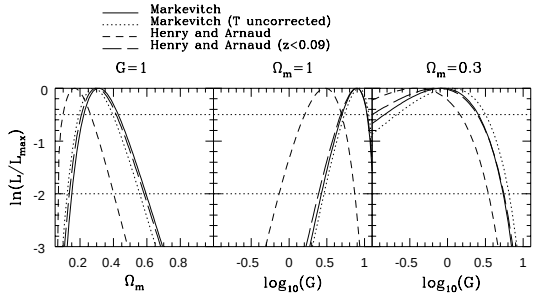

FIG. 4.— Likelihood (marginalized over σ_8) for the $0.65 < z < 0.9$ data combined with different low redshift data, as labeled. The dotted horizontal lines show likelihood thresholds corresponding to 1σ (top line) and 2σ (bottom line) confidence limits.

The likelihood functions are almost identical (in particular, the temperature corrections in the Markevitch sample make very little difference), with the exception of the Henry and Arnaud data without a volume limit. The difference in this case arises because the hottest clusters in the sample are luminous enough to be visible at redshifts larger than $z = 0.09$. For instance, the hottest cluster in the sample (A2142) is sufficiently luminous to be detected out to a redshift of 0.014, implying $V_{\rm max} = 1.6 \times 10^8 h^{-3}{\rm Mpc}^3$, while the imposition of the redshift limit reduces $V_{\rm max}$ to $4.6 \times 10^7 h^{-3}{\rm Mpc}^3$. Similar changes in $V_{\rm max}$ apply to the two next most luminous clusters, implying that the three brightest clusters are all found within the closest 1/3 of the volume in which they could be detected. The fact that no clusters are actually observed at $z > 0.09$ in this sample is either a chance occurrence (the event has moderate statistical significance) or suggests that either the luminosity-temperature relation or the number abundance of clusters evolves significantly beyond $z = 0.09$. The latter two effects would invalidate our analysis, since we do not take into account any evolution within a single redshift bin. However, this problem can be eliminated by making sure the redshift bin is sufficiently small, for instance by limiting the maximum redshift. The imposition of a volume limit does indeed yield results which are in extremely close agreement with those from the Markevitch sample, and we make use of the Markevitch data to normalize the low redshift cluster abundance for most of the remaining discussion.

Second, we consider the effect of using different high redshift datasets. Fig.5 shows the likelihood (marginalized over σ_8) for three different choices of high redshift data, for the cases $G = 1$, $\Omega_m = 1$, and $\Omega_m = 0.3$. The Henry data contains the most clusters and is the best understood systematically, as it is complete to a known flux limit. However, even the most extreme models are not expected to show very much evolution at this moderate redshift, and very little of the available parameter space is ruled out at the 2σ level. The constraints from the two clusters in the interval $0.5 < z < 0.65$ are somewhat stronger, with $\Omega_m = 1$ with gaussian fluctuations being inconsistent at the 2σ level. However, the greatest statistical weight comes from the highest redshift sample, despite the fact that it contains only one cluster. (Henceforth we consider a model to be inconsistent at the 2σ level if $\ln(L/L_{\rm max}) < -2$, and at the 1σ level if $\ln(L/L_{\rm max}) < -0.5$, which are the thresholds which would apply if the likelihood function were gaussian – most of our likelihood functions are close to Gaussian at their peak, so this approximation should be reasonable. These thresholds are shown by horizontal lines in our likelihood plots).

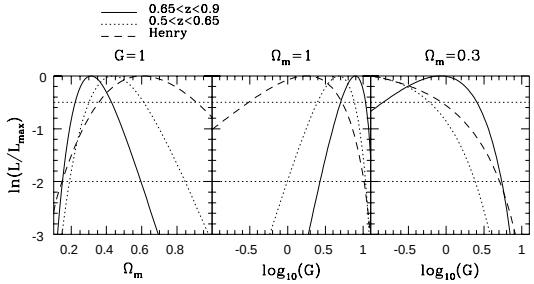

FIG. 5.— Likelihood (marginalized over σ_8) for the Markevitch data, combined with different high redshift data, as labeled. The dotted horizontal lines show likelihood thresholds corresponding to 1σ (top line) and 2σ (bottom line) confidence limits.

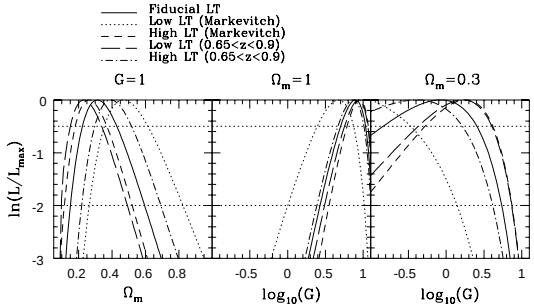

FIG. 6.— Likelihood (marginalized over σ_8) for the Markevitch data and the $0.65 < z < 0.9$ data under different assumptions about the cluster luminosity-temperature relationship, as discussed in the text. The dotted horizontal lines show likelihood thresholds corresponding to 1σ (top line) and 2σ (bottom line) confidence limits.

Next we investigate the effect of uncertainties in the LT relation on the allowed ranges of Ω_m and G. Fig.6 shows the likelihood for a variety of choices of LT relationship at low and high redshifts. As noted, we have attempted to restrict our analysis to temperatures which are sufficiently high that volume limits are more important than flux limits, thus minimizing the importance of the LT relation. We see from the figures that changing the LT relation at high redshift has relatively little effect on the likelihood function. The only change that makes a significant difference is reducing the amplitude of the LT relationship

at low redshift. Such a change would imply that the true number density of clusters of a given temperature is in fact higher, increasing the inferred level of cluster evolution and increasing the preferred value of Ω_m (or reducing the preferred value of G in the non-gaussian case). However, even for the extreme case considered here, where the mean luminosity is reduced by a factor of 2, the changes to the likelihood function are not large.

Now we investigate the effect of uncertainties in the measured temperature of the high redshift cluster MS1054.5-0321. In fig.7 we show the likelihood function marginalized over σ_8 for the cases $G = 1$, $\Omega_m = 1$, and $\Omega_m = 0.3$ under four different assumptions about the true temperature of the cluster ($T = 10.0$keV, $T = 12.0$keV, $T = 14.7$keV and $T = 16.0$keV). Assuming an $M_{<R} \propto R^{0.64}$ cluster profile, the corresponding masses within a 1.5Mpc comoving radius are $0.62 \times 10^{15} h^{-1} M_\odot$, $0.76 \times 10^{15} h^{-1} M_\odot$, $0.96 \times 10^{15} h^{-1} M_\odot$ and $1.06 \times 10^{15} h^{-1} M_\odot$ respectively if $\Omega_m = 1$, and $0.70 \times 10^{15} h^{-1} M_\odot$, $0.86 \times 10^{15} h^{-1} M_\odot$, $1.09 \times 10^{15} h^{-1} M_\odot$ and $1.20 \times 10^{15} h^{-1} M_\odot$ respectively if $\Omega_m = 0.3$. These possibilities span the range allowed by other estimates of the mass of the cluster from weak lensing and velocity dispersion observations (Bahcall & Fan 1998a). For lower cluster temperatures, the preferred value of Ω_m is higher (or in the non-gaussian case the preferred value of G is higher). However, even for the lowest value of T considered, an $\Omega_m = 1$ universe with gaussian fluctuations is inconsistent at the 2σ level, with the best fit value of Ω (or G in the non-gaussian case) almost unchanged.

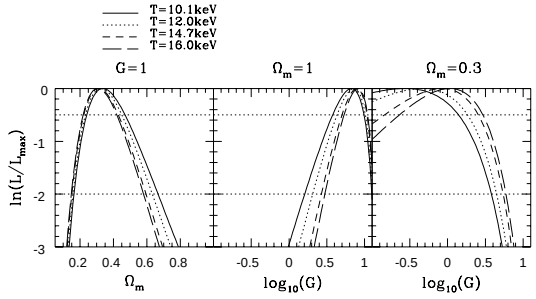

FIG. 7.— Likelihood (marginalized over σ_8) for the Markevitch data and the $0.65 < z < 0.9$ data, under different assumptions about the temperature of MS1054.5-0321. The dotted horizontal lines show likelihood thresholds corresponding to 1σ (top line) and 2σ (bottom line) confidence limits.

Next we consider the effect of varying the range of temperatures $T_{\rm min} < T < T_{\rm max}$ over which we perform our likelihood analysis for the high redshift sample. In fig.8 we show the likelihood function marginalized over σ_8 for the cases $G = 1$, $\Omega_m = 1$, and $\Omega_m = 0.3$ for $T_{\rm min} = 6.3$keV, $T_{\rm min} = 10.0$keV, and $T_{\rm min} = 14.0$keV. For lower values of $T_{\rm min}$ it becomes increasingly more likely that the $0.65 < z < 0.9$ sample is incomplete, as there are fainter clusters in this redshift range whose temperatures have not yet been measured. Our analysis assuming $T_{\rm min} = 6.3$keV probably underestimates the true number of clusters in this temperature range (which it takes to be one), and therefore over-estimates the degree of cluster evolution, consequently over-estimating Ω_m (or underestimating G in the gaussian case). Our analysis assuming $T_{\rm min} = 14$keV is less likely to be subject to incompleteness. However, in the case that the true temperature of MS1054.5-0321 turned out to be less than 14keV, our sample would have over-estimated the number of clusters within the temperature range (as one instead of zero), making the analysis invalid. The case $T_{\rm min} = 10.0$keV lies in the middle, and the two cases just discussed can be considered to represent a wide range of systematic error from incompleteness of the high redshift sample. In the gaussian case, the best fit value of Ω_m is in the range $\Omega_m = 0.3 \pm 0.15$, but no choice of $T_{\rm min}$ is able to reconcile a gaussian $\Omega_m = 1$ universe with the data at the 2σ level.

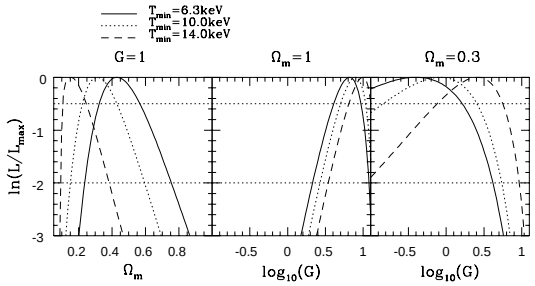

FIG. 8.— Likelihood (marginalized over σ_8) for the Markevitch data and the $0.65 < z < 0.9$ data, for different values of the parameter $T_{\rm min}$. The dotted horizontal lines show likelihood thresholds corresponding to 1σ (top line) and 2σ (bottom line) confidence limits.

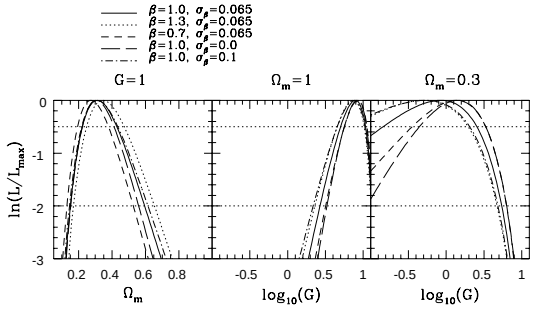

FIG. 9.— Likelihood (marginalized over σ_8) for the Markevitch data and the $0.65 < z < 0.9$ data, for different versions of the mass-temperature relationship. The dotted horizontal lines show likelihood thresholds corresponding to 1σ (top line) and 2σ (bottom line) confidence limits.

Next we consider the effect of changes in the mass temperature relationship on our likelihood analysis. Fig.9 shows the likelihood function marginalized over σ_8 for the cases $G = 1$, $\Omega_m = 1$, and $\Omega_m = 0.3$ for different values of the parameters β and σ_β. The maximum likelihood values and exclusion limits are not significantly changed by

any of these modifications. Also, we consider the effect of varying the power spectrum of the fluctuations. Fig.10 shows the likelihood function marginalized over σ_8 for the cases $G = 1$, $\Omega_m = 1$, and $\Omega_m = 0.3$ and a CDM shape parameter Γ in the range $0.05 < \Gamma < 0.5$, wide enough to encompass any viable model. Exclusion limits are not significantly altered by variations of Γ in this range.

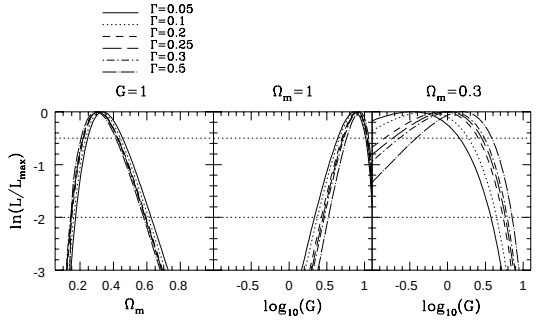

FIG. 10.— Likelihood (marginalized over σ_8) for the Markevitch data and the $0.65 < z < 0.9$ data, for different values of the power spectrum shape parameter Γ. The dotted horizontal lines show likelihood thresholds corresponding to 1σ (top line) and 2σ (bottom line) confidence limits.

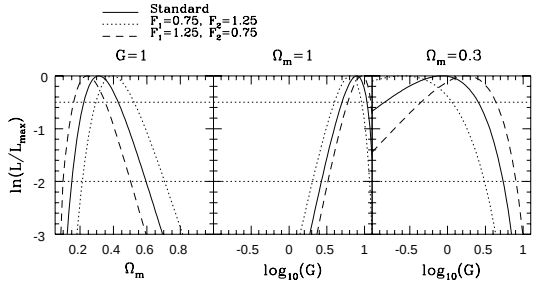

FIG. 11.— Likelihood (marginalized over σ_8) for the Markevitch data and the $0.65 < z < 0.9$ data, for different values of the parameters F_1 and F_2, included to account for possible systematic errors in the Press-Schechter prediction for non-gaussian models. The dotted horizontal lines show likelihood thresholds corresponding to 1σ (top line) and 2σ (bottom line) confidence limits.

Now we consider the effect of possible systematic errors in the modified Press-Schechter prediction for non-gaussian models. Robinson & Baker (1999) have shown that the Press-Schechter formula can model the number abundance of clusters observed in n-body simulations with non-gaussian initial conditions to better than 25% accuracy. We test the effect of this degree of systematic uncertainty by multiplying the low and high redshift predictions of the cluster number abundance by factors F_1 and F_2 respectively. Fig.11 shows the likelihood function marginalized over σ_8 for the standard choice $F_1 = F_2 = 1$, a model with enhanced evolution for which $F_1 = 1.25$ and $F_2 = 0.75$, and a model with less evolution, for which $F_1 = 0.75$ and $F_2 = 1.25$. Increasing the degree of evolution slightly increases the preferred value of Ω_m, or reduces the preferred value of G in the non gaussian case, and decreasing the degree of evolution has a small effect in the opposite direction. Even in this extreme case however, where we have changed the relative number densities at low and high redshift by a factor of more than 50%, considerably more than the uncertainty suggested by the simulations of Robinson & Baker, there is little effect on the results of our likelihood analysis.

Finally, we show the effect of assuming a flat universe with a cosmological constant, rather than the open case which we have considered up to now. Fig.12 shows the likelihood function marginalized over σ_8 for the cases $G = 1$, $\Omega_m = 0.3$, and $\Omega_m = 0.6$ for open and flat universes. The lambda case typically predicts slightly more evolution than the open case if the other parameters are held fixed. Consequently, the best fit values of Ω_m are slightly lower, or in the non-gaussian case, the best fit value of G is slightly higher.

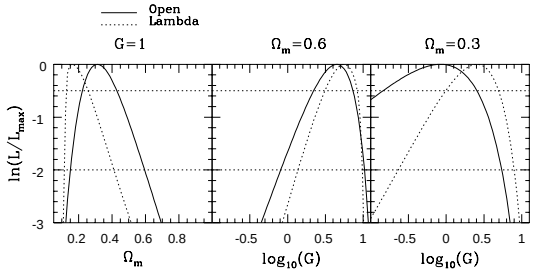

FIG. 12.— Likelihood (marginalized over σ_8) for the Markevitch data and the $0.65 < z < 0.9$ data, for open and flat universes. The dotted horizontal lines show likelihood thresholds corresponding to 1σ (top line) and 2σ (bottom line) confidence limits.

Having considered the importance of various sources of systematic error, we now show the likelihood function derived by combining all of the cluster data at different redshifts. In Fig.13 we show the likelihood function (marginalized over σ_8) for the cases $G = 1$, $\Omega_m = 1.0$ and $\Omega_m = 0.3$, using the combination of the Markevitch, Henry, $0.5 < z < 0.65$ and $0.65 < z < 0.9$ datasets. We show the results for open and flat universes together with two additional analyses for the open case. The first, denoted "Low Ω", incorporates the major systematic uncertainties favoring a low value of Ω_m. The second, denoted "High Ω"), incorporates the major systematic uncertainties favoring a high value of Ω_m. For the "Low Ω" model, we replace the Markevitch data at low redshift with the Henry and Arnaud sample, without a volume limit, and we adopt a lower temperature bound of $T_{\rm min} = 14.0$keV for our analysis of the $0.65 < z < 0.9$ sample. For the "High Ω" model, we multiply the Press-Schechter prediction for the low redshift sample by a factor $F_1 = 0.75$, and the predictions for the $0.5 < z < 0.65$ and $0.65 < z < 0.9$ samples by a factor $F_2 = 1.25$. We also adopt a normalization for

the mass-temperature relationship of $\beta = 1.3$, use a temperature for MS1054.5-0321 of 10.1keV, and adopt a lower temperature bound of $T_{\rm min} = 6.3$ for the analysis of the $0.65 < z < 0.9$ sample. The results from the "High Ω" and "Low Ω" analyses span a reasonable range of systematic uncertainty in the true likelihood function. To summarize the results of the full likelihood analysis, we we find that for a gaussian universe, the best fit value of Ω_m is in the range $\Omega_m \simeq 0.4 \pm 0.25$, with $\Omega_m = 1$ inconsistent at the 2σ independent of almost all sources of systematic error. The gaussian, $\Omega_m = 1$ case can only be reconciled at the 2σ level by a conspiracy of several systematic effects working in the right direction. If we assume that $\Omega_m = 1$, then the predicted degree of cluster evolution can be reconciled with the observations if $G > 2.0$, with the best fit value being $G \simeq 6.5 \pm 2.0$. Under the assumption that $\Omega_m = 0.3$, gaussianity is always consistent with the data, but a wide range of non-gaussian models also fit, with all values $G < 4$ (or $G < 6$ in the lambda case) acceptable at the 2σ level. These conclusions are robust to a wide range of systematic uncertainties, and independent of whether the universe is open or flat.

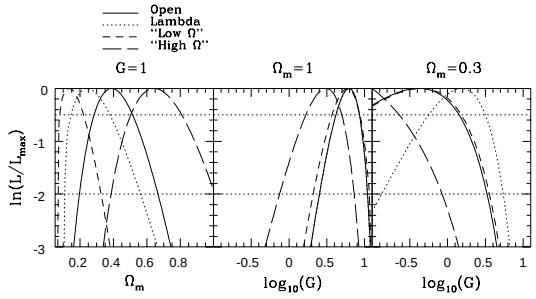

FIG. 13.— Likelihood (marginalized over σ_8) for all datasets combined, for an open universe, a lambda universe, and for "Low Ω" and "High Ω" analyses which incorporate a number of systematic effects favoring low and high values of Ω_m respectively. The dotted horizontal lines show likelihood thresholds corresponding to 1σ (top line) and 2σ (bottom line) confidence limits.

We discuss briefly the degree of non-gaussianity which these G values represent. Fig.14 shows probability distribution functions with $G = 1$, $G = 2.5$ and $G = 9$. We see that the gaussian and the $G = 2.5$ cases are barely distinguishable, with the differences only becoming apparent for the rare tail of fluctuations. We reiterate that the level of non-gaussianity represented by the $G = 2.5$ PDF is sufficient to reconcile an $\Omega_m = 1$ universe with the observed degree of cluster evolution. The $G = 9$ PDF differs from the gaussian case more obviously over its entire range, not just for the rare tail of perturbations. We can also relate the parameter G to some more familiar characterizations of non-gaussianity. In Fig.15, we show the relationship between skewness S, kurtosis K, and non-gaussianity parameter G for the log normal family of PDFs we are considering. Since the PDF is normalized to have mean zero and standard deviation one, the skewness is just

$$S = \int_{-\infty}^{\infty} y^3 P(y)\, dy. \tag{24}$$

while the kurtosis is

$$K = \int_{-\infty}^{\infty} y^4 P(y)\, dy\, - 3. \tag{25}$$

The $G = 2.5$ case has a skewness of 0.3, and a kurtosis of 0.1, while the $G = 9.0$ case has a skewness of 1.2 and a kurtosis of 2.6. Some typical G values for physical models are: cosmic strings – $G \simeq 5$ (Robinson & Baker 1999), cosmic textures – $G \simeq 14$ (Park, Spergel & Turok 1989), Peebles ICDM $G \simeq 15$ (Robinson & Baker 1999). The latter two models would therefore appear to be ruled out if the matter density of the universe is of order 0.3.

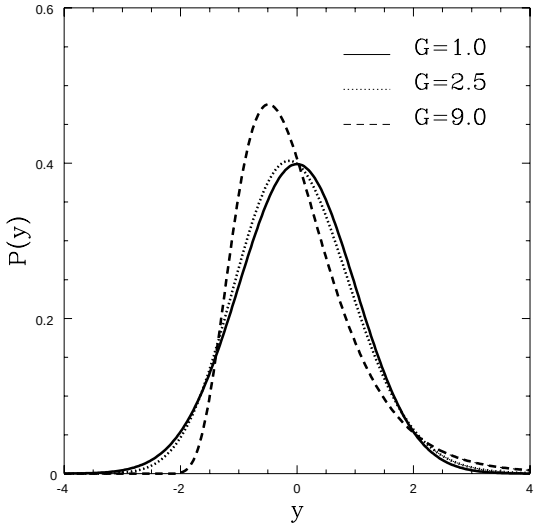

FIG. 14.— A gaussian and two non-gaussian PDFs, with non-gaussianity parameters as labeled.

From this discussion, we see that the level of non-gaussianity required to reconcile an $\Omega_m = 1$ universe with existing cluster evolution data is relatively small, and less than the amount predicted by many well motivated non-gaussian models. One promising scenario which could 'save' $\Omega_m = 1$ is a special form of "hybrid inflation", where an initial spectrum of adiabatic gaussian fluctuations is further perturbed by the evolution of a network of cosmic defects (Contaldi, Hindmarsh & Magueijo 1999; Battye & Weller 1998). The level of non-gaussianity in such a model would be lower than that resulting from the action of the defect network alone. Of course, for this model to work it would also have to overcome a number of independent arguments against a critical density universe (see e.g. Bahcall & Fan 1998b).

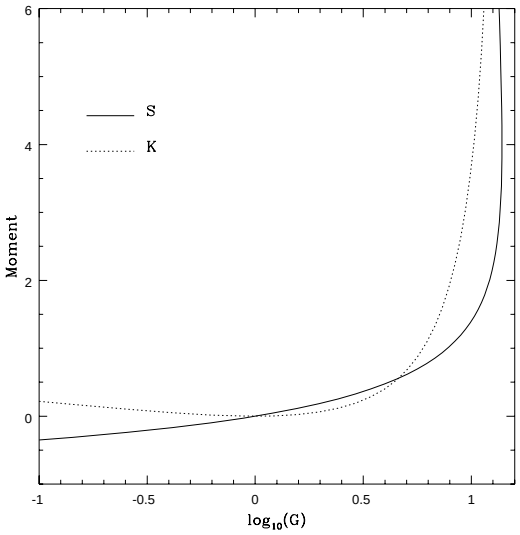

FIG. 15.— The relationship between skewness and non-gaussianity parameter G for the log-normal family of PDFs.

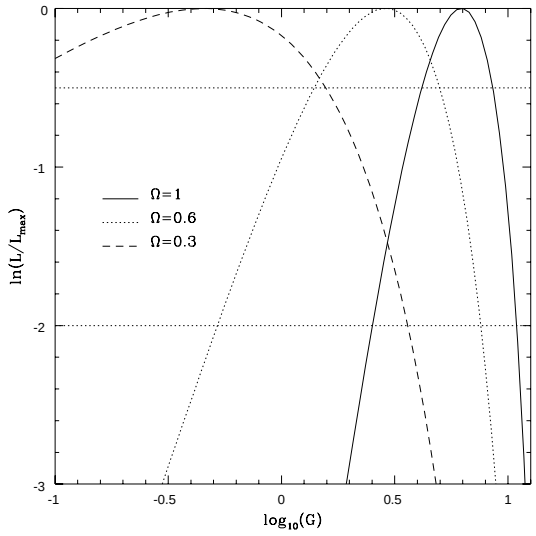

FIG. 16.— Likelihood (marginalized over σ_8) for the three models discussed in section 4.2 and the combination of the Markevitch and $0.65 < z < 0.9$ datasets. The models are labeled by the value of Ω_m, and analyzed assuming that the true value of Ω_m has been measured precisely in each case. The dotted horizontal lines show likelihood thresholds corresponding to 1σ (top line) and 2σ (bottom line) confidence limits.

4.2. *Future data*

We have seen that existing cluster evolution data strongly disfavors an $\Omega_m = 1$ universe with gaussian fluctuations, preferring either a low value of Ω_m, or a high value of G. An independent measure of Ω_m (from CMB data and supernovae observations for example) would therefore allow us to draw conclusions about the degree of non-gaussianity in the universe. Let us consider three different models which are roughly degenerate with respect to current cluster data: a model with $\Omega_m = 1.0$, $G = 8.0$, $\sigma_8 = 0.35$, a model with $\Omega_m = 0.6$, $G = 4.5$, $\sigma_8 = 0.525$, and a model with $\Omega_m = 0.3$, $G = 1.0$, $\sigma_8 = 0.85$. The likelihood function of these models relative to the observational data considered above is shown in fig.16. To evaluate these likelihood functions, we have assumed that Ω_m is measured to within 0.05 for the $\Omega_m < 1$ cases, and then marginalized over this uncertainty. For the $\Omega_m = 1.0$ model, assuming that we have an unambiguous determination of the true value of Ω_m, the current cluster data gives a clear detection of the non-gaussianity of the fluctuations, as discussed above. For the $\Omega_m = 0.6$ model, the current observational data is unable to detect the non-gaussianity, with gaussian fluctuations allowed at the 2σ level. For the $\Omega_m = 0.3$ case, gaussian fluctuations are consistent with the data, with the non gaussianity parameter constrained to be $G < 4.0$ at the 2σ level.

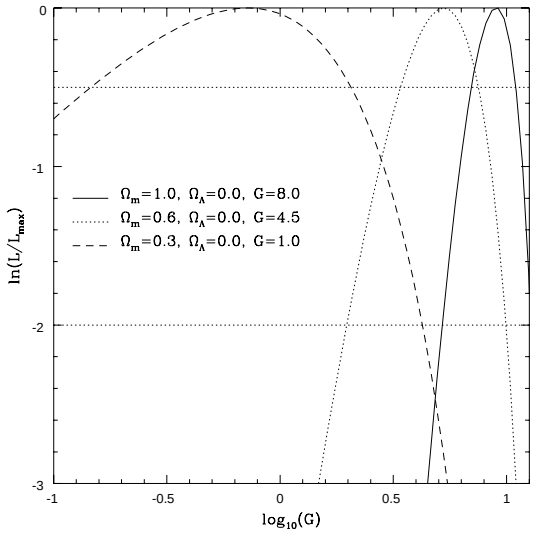

FIG. 17.— Mock likelihood functions (marginalized over σ_8) for the three models discussed in section 4.2 and the combination of the Markevitch and EMSS *mock* datasets. The models are labeled by the value of Ω_m, and analyzed assuming that the true value of Ω_m has been measured (plus or minus errors of 0.05 in the $\Omega_m < 1$ cases). The dotted horizontal lines show likelihood thresholds corresponding to 1σ (top line) and 2σ (bottom line) confidence limits.

For each of the models just mentioned, we have also computed likely confidence limits which could be achieved by a considerable but realistic increase in the volume of cluster evolution data. For each model, we have generated mock realizations of the Markevitch catalogue, and of a complete EMSS catalogue, assuming that temperatures are measured for all clusters within the EMSS survey for which $T > 6.3$keV and $z < 0.9$. To generate these catalogues, we split the surveys into a number of redshift slices (one slice for the Markevitch data, with the same redshift and flux limits, and the same sky coverage, and four slices for the EMSS data with $0.3 < z < 0.4$, $0.4 < z < 0.5$, $0.5 < z < 0.65$, and $0.65 < z < 0.9$, assuming the sky cov-

erage and flux limits of the EMSS survey). For each slice, we compute the mean volume surveyed for each cluster temperature, assuming the fiducial LT relationships given above. We then generate a Poisson sample of clusters satisfying the $n(T)$ law for the model in question, computed at the median redshift of the sample.

We now assume that the true value of Ω_m has been measured, by some independent method (to plus or minus 0.05, except for the $\Omega_m = 1$ case, where we assume an exact determination), and ask how well the mock catalogues are able to constrain the non-gaussianity parameter G. Results for the likelihood function (marginalized over σ_8, which is unknown, and the uncertainty in Ω_m) are shown in fig.17. In the $\Omega_m = 1$ case the improved data considerably reduces the errors on the determination of G, and in the $\Omega_m = 0.6$ case an unambiguous detection of non-gaussianity would be possible at the 2σ level. In the $\Omega_m = 0.3$ case, the allowed range of G is not significantly reduced, with the limit still being $G < 4$ at the 2σ level.

From the above discussion, we see that even the considerable improvement in the quantity of cluster data discussed above would not significantly improve constraints on non-gaussianity if Ω_m is really of order 0.3. The reason cluster evolution does not give us such strong constraints in this case is that in a low density universe, clusters are not such rare events. For this reason, they do not probe the high-σ tail of the PDF, which is where gaussian and non-gaussian PDFs tend to differ most significantly. This fact is illustrated in fig.18, where we show the cumulative number density of clusters expected at redshifts $z = 0.05$, $z = 0.8$, $z = 1.5$ and $z = 2.0$ for two models of structure formation (gaussian – $G = 1.0$, $\sigma_8 = 0.85$, and non-gaussian – $G = 3.0$, $\sigma_8 = 0.75$), both with $\Omega_m = 0.3$, which are nearly degenerate with respect to the real and mock data discussed above. We see that the degree of evolution between $z = 0.05$ and $z = 0.8$ begins to differ considerably between the two models only for cluster temperatures larger than about 20keV. However, clusters this hot are so rare ($N_{>T} < 10^{-10} h^3 \mathrm{Mpc}^{-3}$) that the surveys considered above do not probe enough volume to place any constraints on the number density. As we move to higher redshifts, lower temperature clusters become rarer, many-σ events, and the degree of evolution to $z = 1.5$ differs considerably between the two models for cluster temperatures of order 15keV. For the non-gaussian model discussed above, the number density of such clusters at redshift $z = 1.5$ is $N_{>15\mathrm{keV}} \simeq 10^{-9} h^3 \mathrm{Mpc}^{-3}$, meaning that a survey sensitive to clusters in the range $1.25 < z < 1.75$ would have to cover approximately 1000 square degrees to find an average of one $T > 15$keV cluster. The existence of such a cluster would however be ten times less in a gaussian universe, where $N_{>15\mathrm{keV}} \simeq 10^{-10} h^3 \mathrm{Mpc}^{-3}$. We conclude therefore, that if the matter density of the universe does indeed turn out to be of order $z = 0.3$, much deeper cluster data will be required to improve constraints on non-gaussianity, with surveys covering 1000 or more square degrees capable of detecting hot clusters ($z > 15$keV) at redshifts $z \geq 1.5$. A catalogue based on serendipitous cluster detections from the forthcoming XMM satellite could hope to cover such an area to sufficient depth (Romer 1998).

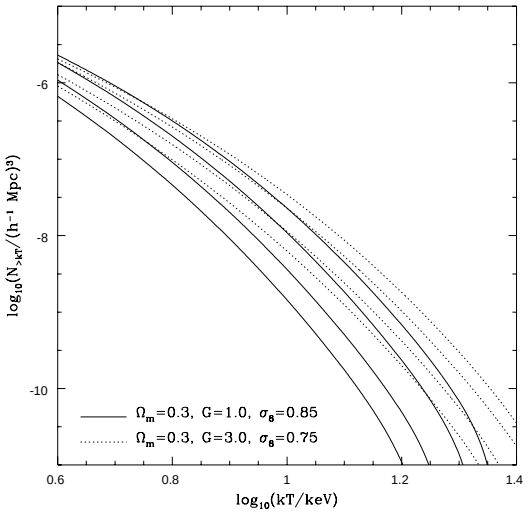

FIG. 18.— Predicted cluster abundances at $z = 0.05$, $z = 0.8$, $z = 1.5$, $z = 2$ (highest to lowest curves, respectively), for a gaussian and a non-gaussian model, as labeled, with Ω_m=0.3.

5. CONCLUSIONS

We have made use of a modified version of the Press-Schechter formalism to examine the constraints on non-gaussianity which can be derived from observations of evolution of the galaxy cluster number abundance. Our results our summarized in Fig.13, which shows likelihood functions for the combined cluster datasets for the cases $G = 1$ (gaussian fluctuations), $\Omega_m = 1$, and $\Omega_m = 0.3$. For an open universe with gaussian fluctuations, the maximum likelihood value of the matter density on the basis of current observations is in the range $\Omega_m \simeq 0.4 \pm 0.25$, with the case $\Omega_m = 1$ inconsistent with the data at the 2σ level. If we assume an $\Omega_m = 1$ universe with non-gaussian fluctuations, the best fit value of the non-gaussianity parameter is in the range $G = 6.5 \pm 2$, with $G > 2.0$ required for consistency with the data at the 2σ level. The degree of non-gaussianity required to 'save' the critical density universe is therefore relatively small, and could easily be realized by physically motivated models such as the combination adiabatic and defect seeded perturbations predicted by some Hybrid inflation models. If we assume an $\Omega_m = 0.3$ universe, the non-gaussianity parameter is constrained to be $G < 4$ ($G < 6$ in the lambda case) at the 2σ level. These conclusions are robust to a wide range of sources of systematic uncertainty. An $\Omega_m = 1$ universe with gaussian fluctuations could only be reconciled with the data if a conspiracy of several systematic errors were to all modify our conclusions in the right direction. In particular, our results are unaffected by possible systematic errors in the Press-Schechter prediction for the cluster abundance in non-gaussian models, which Robinson & Baker have shown to be less than 25%. Our conclusions are also largely independent of whether the universe is open or flat (slightly lower values of Ω_m or higher values of G are preferred in the cosmological constant case). Since the non-gaussian Press-Schechter formalism requires only the

probability distribution function of primordial fluctuations as input, our analysis is independent of any uncertain features of the non-gaussian physics in specific models.

The techniques discussed here allow us to constrain primordial non-gaussianity in the universe, provided we have an independent measurement of the matter density Ω_m. We can realistically expect to gain such a measurement with high precision from the combination of upcoming CMB and supernovae data. If the matter density is measured to be $\Omega_m = 1$ then the current cluster evolution data represents a detection of non-gaussianity. If the matter density is measured to be $\Omega_m = 0.6$ or lower then both gaussian and non-gaussian fluctuations are consistent with current cluster evolution data.

Our results for the Gaussian case agree well with those of Bahcall & Fan (1998a) who find $\Omega_m = 0.2^{+0.3}_{-0.1}$ and Eke et al. (1998) who find $\Omega_m = 0.45 \pm 0.2$, each using similar data to that considered here. Our results disagree however with those of Blanchard & Bartlett, who find evidence in favor of an $\Omega_m = 1$ universe by combining the EMSS and ROSAT samples. As for non-gaussian models, our results are consistent with those of Willick (1998) in that both studies allow for a significant degree of non-gaussianity if $\Omega_m \simeq 0.3$. Our analysis however does not significantly disfavor gaussianity in this case. This difference is probably due to the fact that we include more clusters and allow for more sources of systematic error, particularly in the low-redshift normalization. Our results are consistent with those of RGS98 and Koyama et al. (1999) provided that the matter density of the universe is low. In particular, RGS98 found that a significant amount of non-gaussianity ($G \simeq 4.0^{+3.6}_{-2.0}$) was required to reconcile cluster abundance and cluster correlation data in the $\Omega_m = 0.3$ case. We caution the reader however that the arguments used in these last two papers depend on a model for halo correlations in non-gaussian models whose agreement with N-body simulations is currently uncertain. On the other hand, the arguments used in the current work, and that of Willick (1998), are based on a model for halo abundance in non-gaussian models which has been shown to agree well with that observed in simulations.

We have also investigated the improvement to constraints on non-gaussianity which we could expect from a realistic increase in the quantity of data. If the matter density of the universe is measured to be high (Ω_m greater than of order 0.6), then a moderate increase in the amount of cluster evolution data will allow a definite detection of non-gaussianity. However, if the matter density is measured to be low, then a substantial increase in the quantity of cluster evolution will be required in order to significantly improve upon the limits derived here. The reason that constraints are weaker in the $\Omega_m = 0.3$ case is that clusters at moderate redshifts ($z \simeq 0.9$) are no longer particularly rare events, while the strongest constraints on gaussianity come from probing the rarest tail of fluctuations. The best prospect for constraining non-gaussianity in this case is to carry out deep surveys capable of detecting hot clusters ($T > 15$keV) at high redshift ($z \geq 1.5$). Such surveys would be able to distinguish a non-gaussian universe with $G = 3$ from a universe with gaussian fluctuations if the area covered was of order 1000 square degrees. Conducting such surveys is a challenge which will deserve considerable attention if the matter density is indeed confirmed to be low.

6. ACKNOWLEDGMENTS

We would like to thank Pat Henry for supplying updated information on the Henry (1997) cluster sample. We would also like to thank Marc Davis for helpful discussions. This work has been supported in part by a grant from the NSF, and E.G. acknowledges partial support from NASA AISRP (NAG-3941).

REFERENCES

Amendola, A., & Borgani, S. 1994, MNRAS, 266, 191
Amendola, A., & Occhionero, F. 1993, ApJ, 413, 39
Arnaud, M., & Evrard, A. E. 1998, astro-ph/9806353
Bahcall, N. A, & Fan, X. 1998a, ApJ, 501, 1
Bahcall, N. A, & Fan, X. 1998b, astro-ph/9804082
Bardeen, J. M., Bond, J. R., Kaiser, N., & Szalay, A. S. 1986, ApJ, 304, 15
Battye, R. A., & Weller, J. 1998, astro-ph/9810203
Blanchard A., & Bartlett, J. G. 1998, A&A, 332, L49
Bond, J. R., Cole, S., Efstathiou, G., & Kaiser, N. 1991, ApJ, 379, 440
Chiu, W. A., Ostriker, J. P., & Strauss, M. A. 1997, ApJ, 494, 479
Colafrancesco S., Lucchin F., Matarrese S. 1989, ApJ, 345, 3
Contaldi, C., Hindmarsh, H., & Magueijo, J. 1999, Phys. Rev. Lett., 82, 2034
Donahue, M. 1996, ApJ, 468, 79
Donahue, M., Gioia, I., Luppino, G., Hughes, J. P., & Stocke, J. T. 1998, ApJ, 412, 479
Eke, V. R., Cole, S., Frenk, C. S., & Henry, J. P. 1998, MNRAS, 298, 1145
Eke, V. R., Navarro, J. F., & Frenk, C. S. 1998, ApJ, 503, 569
Evrard. A. E., Metzler, C. A., & Navarro, J. F. 1996, ApJ, 469, 494
Fan, X., Bahcall, N. A, & Cen, R. 1997, ApJ, 490, L123
Frenk, C. S., White, S. D. M., Efstathiou, G., & Davis, M. 1990, ApJ, 351, 10
Gross, M. A. K., Somerville, R. S., Primack, J. R., Borgani, S., Girardi, M. 1997, astro-ph/9711035
Kaiser, N. 1986, MNRAS, 222, 323
Kibble, T. W. B. 1976, J. Phys., A9, 1387
Kitayama, T., & Suto, Y. 1996, ApJ, 469, 480
Koyama, K., Soda, J., & Taruya, A. 1999, astro-ph/9903027
La, D. 1991, Phys. Rev. B, 265, 232
Markevitch, M. 1998, ApJ, 504, 27
Mushotzky, R. F. & Scharf, C. A. 1997, ApJ, 482, L13
Navarro, J. F., Frenk, C. S., & White, S.D.M. 1995, MNRAS, 275, 720
Oukbir, J., Blanchard A. 1992, A&A, 262, L92
Oukbir, J., Blanchard A. 1997, A&A, 317, 1
Oukbir, J., Bartlett, J. G., Blanchard A. 1997, A&A, 320, 365
Park, C., Spergel, D. N., & Turok, N. 1991, ApJ, 372, L53
Peebles, P. J. E. 1983, ApJ, 274, 1
Peebles, P. J. E. 1997, ApJ, 483, L1
Peebles, P. J. E., 1998, astro-ph/9805194
Peebles, P. J. E., 1998, astro-ph/9805212
Press, W. H., & Schechter, P. 1974, ApJ, 187, 425
Reichart, D. E., Nichol, R. C., Castander, F. J., Burke, D. J, Romer, A. J., Holden B. P., Collins, C. A., Ulmer, M. P. 1998, astro-ph/9802153
Robinson, J., & Baker, J. E. 1999, astro-ph/9905098
Robinson, J., Gawiser, E., & Silk, J. 1998, astro-ph/9805181
Romer, A. K. 1998, in Wide Field Surveys in Cosmology, ed. Y. Mellier & S. Colombi (Paris: Edition Frontieres)
van de Bruck, C. 1998, astro-ph/9810409
Viana, P. T. P., & Liddle, A. R. 1998, astro-ph/9803244
Vilenkin, A., & Shellard, E. P. S. 1994, Cosmic strings and other topological defects (Cambridge: Cambridge Univ. Press)
Willick, J. 1999, astro-ph/9904367